A SUMMARY OF V/STOL INLET ANALYSIS METHODS

Danny P. Hwang and John M. Abbott
National Aeronautics and Space Administration
Lewis Research Center
Cleveland, Ohio 44135

Abstract

The methods used to analyze the aerodynamic performance of V/STOL inlets at the NASA Lewis Research Center are briefly described. Recent extensions and applications of the method are emphasized. They include the specification of the Kutta condition for a slotted inlet, the calculation of suction and tangential blowing for boundary layer control, and the analysis of auxiliary inlet geometries. A comparison is made with experiment for the slotted inlet and also for tangential blowing. Finally, an optimum inlet diffuser velocity distribution is developed.

Nomenclature

C_f	skin friction coefficient
C_p	pressure coefficient
D	fan diameter
L	inlet length (0.3048 m)
M	Mach number
$\dot{m}$	mass flow rate
P	total pressure
S	surface distance
S.P.	stagnation point
V	velocity
x	x-coordinate
y	y-coordinate
$\bar{x}$	nondimensional distance from the start of diffusion normalized by the total diffusion length
α	angle of attack
β	inlet yaw angle
δ	displacement thickness
θ	circumferential angle ($\theta = 0^o$ at windward plane)

Subscripts:

B	blowing plenum
c	control station
de	diffuser exit
e	edge of the boundary layer
inlet	inlet
j	blowing jet
max	maximum
ref	reference
suction	suction
T	throat
∞	free stream
FAN	fan face

Introduction

In recent years, many different airframe/engine configurations have been proposed for V/STOL aircraft. Some of the proposed configurations impose rather severe flow conditions on the propulsion system inlet. For example, the approach and takeoff flight paths of a tilt nacelle V/STOL aircraft may result in inlet angles of attack up to 120^o. A major concern for the inlet designer at these conditions is the possibility of inlet internal flow separation. Separation free flow is desired to minimize thrust loss, minimize fan blade stress, and prevent engine stall. To assist the designer in providing inlet designs with separation-free flow, reliable theoretical methods of inlet flow analysis are desired both for the inlet design process and to interpret and augment the results of wind tunnel testing. The methods should be able to calculate the potential and boundary layer flows in inlets of arbitrary geometry and at arbitrary flow conditions.

Such methods of analysis have been developed over the past several years at the NASA Lewis Research Center. They consist of a series of computer programs documented in Refs. 1 to 6. Comparisons with experimental results are presented in Refs. 7 to 12. Since these reports have been published, the programs have been extended and applied to more difficult inlet problems.

The present paper will briefly describe the basic method of analysis. The major emphasis, however, will be on presenting the recent extensions and applications. The topics covered in this paper are: the flow about a slotted inlet; the flow in an auxiliary inlet; the analysis of suction and blowing boundary layer control; and the development of an optimum diffuser velocity distribution.

Basic Method of Analysis

The basic problem to be solved is to calculate the compressible viscous flow in inlets of arbitrary geometry and at arbitrary operating conditions. A series of computer programs developed at the NASA Lewis Research Center are used to solve this problem. A flow chart depicting the sequence for using these programs is presented in Fig. 1 with the basic programs on the left, and recent extensions on the right. All programs start with the geometry program, upper left-hand block, which creates the discrete control points for each geometric configuration. Then the incompressible potential flow program is used to calculate the basic solutions to the problem. These basic solutions are combined into a solution that satisfies the inlet operating conditions of freestream velocity, angle of attack, and inlet mass flow. Next, the imcompressible flow is corrected for compressibility effects. The compressible potential flow solution is then used as an input to the boundary layer program which calculates the laminar, transition and turbulent boundary layer characteristics, and predicts flow separation.

Two iteration loops are available as shown to the left in Fig. 1. The first adds the displacement thickness to the geometry to improve the accuracy of the potential flow and boundary layer calculations. The second incorporates an automatic angle of attack sweep to find the separation angle of attack of an inlet at any given value of freestream velocity and inlet mass flow in one uninterrupted computer run.

The recent extensions to these programs, which will be the major emphasis of this paper are: (a) to calculate the flow in an inlet with a leading edge slot; (b) to calculate the performance of suction and tangential blowing boundary layer control concepts, and (c) to analyze the flow in auxiliary inlet geometries. The method has also been applied to finding the optimum velocity distribution in a subsonic diffuser.

Geometry Program

A program called SCIRCL is used for 2-D and axisymmetric geometries. For an axisymmetric inlet case, the geometry is represented by its meridional profile which is shown in Fig. 2(a). Both the external and internal ducts are extended far downstream so that accurate potential flow solution can be obtained in the region of interest. SCIRCL breaks the profile into segments with a control point on each segment which are used for potential flow calculations. The program also calculates information such as curvature, wall angles, and flow area distribution which are very useful in preliminary screening of proposed inlet shapes. In addition to the surface points, SCIRCL generates off body points (like flow measuring rakes) also shown in Fig. 2(a) at axial locations where the velocity profile or the streamlines are desired.

The 3-D geometry program, applicable to inlet geometries like that shown in Fig. 2(b) and discussed in Ref. 13, allows the user to input a relatively small number of points to define the inlet and centerbody. The routine then enriches the point number and redistributes the points for good potential flow analysis. The detailed description of this geometry package is given in Ref. 5.

Incompressible Potential Flow Basic Solutions

The Douglas Neumann Program[5,14-16] is used for calculating the incompressible potential flow field. The following basic solutions are obtained by this program:

1. Static solution ($V_\infty = 0$)
2. Uniform axial flow solution
3. 90° angle of attack solution
4. 90° angle of yaw solution (for 3-D geometry only)

In general, to obtain the basic solutions, the surface is replaced by a number of panels on which there is a surface source (or sink) distribution of unknown strength. For 2-D and axisymmetric cases, the source density can be a constant, linear or parabolic. For the 3-D case, only a constant source density can be used. The strength of source distribution varies over the surface in a manner such that at every control point the normal velocity is zero. The best static solution is found to result from using a vorticity distribution on the cowl surfaces (as opposed to a source or sink distribution).

Linear Combination and Corrections

The basic solutions obtained from the incompressible potential flow calculation are combined linearly into a solution of interest having arbitrary flow conditions of free stream velocity, mass flow rate, and angle of attack.[17] In cases where a Kutta condition is required, the constants for linear combination are readjusted to satisfy the Kutta condition. The linearly combined incompressible solution is then corrected for compressibility.[18] If the local velocity is supersonic, it is further corrected by an empirical supersonic correction formula.[19] The final potential flow solution can now be used as an input to the boundary layer program.

Boundary Layer

The analysis of the boundary layer uses a 2-dimensional compressible boundary layer program. The complete documentation of the boundary layer program is given in Ref. 6. The program calculates important boundary layer parameters such as displacement thickness, momentum thickness, and skin friction coefficient, C_f. It also provides the boundary layer velocity profiles at any desired station. The location of transition from laminar to turbulent flow can either be predicted by the program or can be specified by the user. Flow separation is defined to occur when the skin friction coefficient becomes zero.

Recent Extensions

The discussion thus far has described the basic method of analysis. Now the discussion will focus on describing the recent extensions which were motivated in part by the following thoughts. It is desirable to design a V/STOL inlet as short and as thin as possible in order to reduce the weight, to reduce the friction drag at cruise, and improve pilot visibility. However, when an inlet is too thin the peak velocity is so high that the subsequent adverse pressure gradient causes the flow to separate at the lip resulting in a low pressure recovery and high distortion. Several ways to help control this possible separation are by the use of an inlet lip slot, the use of auxiliary inlets, by suction or blowing boundary layer control, or by optimizing the surface pressure distribution. The analysis techniques to analyze these possibilities are considered next, starting with the slotted inlet.

Slotted Inlet

An axisymmetric slotted inlet is shown in Fig. 3. Two cases are considered, zero degrees angle of attack and angle of attack. At zero degrees angle of attack or at zero forward velocity for an axisymmetric geometry the flow is axisymmetric and specifying the Kutta condition (i.e., the flows from the upper surface and the lower surface join smoothly at the trailing edge.) at one circumferential location is equivalent to specifying the Kutta condition around the entire circumference of the slat. Calculations were made for static conditions, $V_\infty = 0$, and the results are shown in Fig. 3. Experimental data are included for comparison. The agreement is quite good on the main inlet cowl surface (points 6 to 9). The agreement between the theoretical and experimental surface velocities is also good on the slat (points 1 to 5). Figure 3 shows that the peak velocities occurs at point 2 on the slat and point 7 on the main cowl. Both peaks are considerably lower than the peak velocity of the inlet without the slot,[19] which is also indicated on the figure. Thus the addition of the slot has unloaded the lip of the thin inlet.

The case of a slotted inlet at an angle of attack is more difficult, because with the present method, the Kutta condition cannot correctly be

imposed at all circumferential positions simultaneously. The Kutta condition can be imposesd locally at one circumferential location, with the inlet at angle-of-attack, by adjusting the mass flow rate through the slot. Results obtained using this approach are shown in Fig. 4. The agreement between theory and experiment at these conditions is quite good, however, it should be noted that the comparison is being made at the 270° circumferential position (side of the inlet). At this particular location, angle-of-attack effects tend to be minimal and in fact the surface velocity distribution does not change much at all as angle-of-attack is increased from 0°. At other circumferential locations, a local specification of the Kutta condition has not been a very successful analysis method and work is now underway to extend the procedures to permit specification of the Kutta condition around the entire circumference of the slat at any angle-of-attack. Extending the method of analysis to include this feature will result in the ability to analyze a new class of inlet geometries, specifically those that employ leading-edge slats and slots.

Auxiliary Inlet

The method of analysis has also been extended to include auxiliary inlet geometries. Auxiliary inlets increase the total inlet flow area thereby reducing the amount of airflow that must be taken into the main inlet. It is another technique for preventing flow separation on cowl lips at static and low flight speed conditions.

An auxiliary inlet on the top of a conventional subsonic inlet and an auxiliary inlet on the top of a supersonic inlet are considered. A conventional subsonic inlet with an auxiliary inlet is shown in Fig. 5. A continuous "N-line" (in the longitudinal direction) is required for the current version of the 3-D potential flow program. When the N-line meets the auxiliary inlet opening, it is rerouted along the side wall of the auxiliary inlet and then proceeds back to the original N-line as shown in Figs. 5(a) and (b). Additional N-lines are added to completely panel the inlet. This particular example required 682 panels to describe the geometry.

Figure 5 also illustrates the technique used to yield the best static solution for an inlet with an auxiliary inlet: Two inlet-duct systems are considered, one with a straight duct and one with a flared duct as shown in Figs. 5(a) and (b). The flared duct induces more flow through the main and auxiliary inlets. The difference between the velocities for the flared inlet and nonflared duct for a free stream uniform flow then provides the static solution. This procedure was adopted because the velocities in the region of an auxiliary inlet were unrealistically large when the vorticity distribution method noted earlier, was used for the static solution.

The computer time for the basic solutions with the 682 panels is quite high, 19 minutes. However, the basic solutions are only computed once and are stored in the computer for later use in obtaining solutions of interest. Subsequent calculations using a linear combination method required only 5 seconds of computer time.

In order to show the effectiveness of an auxiliary inlet for reducing the inlet peak velocity, a calculatiion was made for a conventional inlet with and without an auxiliary inlet as shown in Fig. 6. The peak velocity ratio is reduced considerably from 3.4 to 2.5 at the highlight of the windward plane when the auxiliary inlet is open which is, of course, the desired result.

The pressure coefficient distribution on the surface around and within an auxiliary inlet is illustrated in Fig. 7 . In this particular case, the results are shown for a supersonic inlet with an auxiliary inlet on the top as illustrated in Fig. 7(a). (This figure also illustrates the hidden line removal feature of the geometry package.) For this case, the Kutta condition is satisfied at the trailing edge of the front surface (point A), and the high velocity occurs at the lower portion of the downstream surface of the auxiliary inlet (point B). By examining pressure distributions of this type, this analysis method can be used to study such variables as the shape, the size, number of, and location of the auxiliary inlets.

Suction and Tangential Blowing

Another recent extension to the basic methods is the analysis of suction and tangential blowing boundary layer control systems. Suction controls the boundary layer by removing that portion of it not having sufficient momentum to negotiate the subsequent adverse pressure gradient. Blowing controls the boundary layer by reenergizing it with a thin jet of high velocity air injected tangentially into the boundary layer.

Some results from this analytical method are shown in Figs. 8 and 9 for suction and blowing, respectively. An axisymmetric inlet having a diffuser exit diameter of 0.508 m was analyzed at a free stream Mach number, $M_\infty = 0.12$, throat Mach number, $M_T = 0.4$, and angle of attack, $\alpha = 60^\circ$. The skin friction coefficient distribution on the internal surface of the windward cowl is shown along with boundary layer velocity profiles at several locations. Without boundary layer control, the solid line, the flow separates at $S/L = 0.81$ where the skin friction coefficient becomes zero. The boundary layer profile, just before separation, is quite weak compared to the one upstream at $S/L = 0.48$. Separation is prevented when the boundary layer is controlled by suction (Fig. 8) - the dashed line. It was necessary to bleed off only 0.12 percent of the inlet mass flow to prevent separation as indicated by the nonzero skin friction coefficients. The static-to-total pressure ratio at the suction location is 0.796.

For the blowing boundary layer control (Fig. 9) a blowing velocity ratio, jet velocity to boundary layer edge velocity, $V_j/V_e = 1.75$ was selected. For this case a blowing mass flow of 0.4 percent of the inlet mass flow was required to maintain attached flow. The reenergized boundary layer is clearly evident in the velocity profile just downstream of the blowing slot.

A comparison of analytical and experimental velocity profiles in the windward plane with blowing being used for boundary layer control was made for 0.508 m axisymmetric inlet at $\alpha = 70^\circ$, $V_T/V_0 = 2$ and $P_B/P_0 = 1.2$. The axial locations of the total pressure rakes used to measure the profiles are shown in Fig. 10. As indicated, the analytical and experimental velocity profiles agree well at the upstream measuring station except in the vi-

cinity of $Y/\delta = 0.375$, where the analytical velocity is too high. This discrepancy between the analytical and experimental results could be the result of the closeness of this measuring station to the blowing slot and the difference between the assumed velocity profile and the experimental velocity profile at the blowing slot exit. A similar trend in blowing velocity profiles was observed in Ref. 20. At the downstream rake location, however, the mixing between blowing jet and boundary layer has already taken place so that the well developed analytical velocity profile agrees very well with the experimental velocity profile.

Next, a comparison of analytical and experimental separation bounds is shown in Fig. 11 for the same inlet. The separation parameter V_T/V_∞ is used to collapse the experimental data. (Refs. 21 and 22). Agreement between the analytical and the experimental separation bounds is found to be excellent up to $\alpha = 80^0$. For angles of attack greater than 80^0, the analytical separation point is predicted to be ahead of blowing slot and the analysis can then not proceed since the boundary layer code cannot perform calculations beyond the separation point.

Optimum Diffuser Velocity Distribution

Another application of the method is concerned with finding the optimum velocity distribution in a subsonic diffuser. This velocity distribution will result in the shortest no-boundary layer control inlet and the lowest loss for the required amount of diffusion.

The design method for an optimum subsonic inlet is given in Refs. 23 and 24. Based on the design criteria given in those references, the boundary layer program was used to find the optimum diffuser velocity distribution. The generalized mathematical form of the velocity distribution is given by

$$V = V_{de} + (V_{max} - V_{de})e^{-5\bar{x}^b}$$

A typical case of $V_{max} = 190$ m/s, $V_{de} = 68$ m/s is shown in Fig. 12. The overall diffusion ratio V_{max}/V_{de} is the same for the three cases shown. The upper part of the figure shows the surface velocity ratio (V/V_{de}) as a function of surface distance s/s_{ref}. Velocity distributions were calculated for three values of the exponent b.

A value of $b = 0.613$ produces the steepest initial velocity gradient (largest initial adverse pressure gradient). The initial adverse pressure gradient is so large that the flow separates on the lip at the beginning of the diffusion process. A value of $b = 1.005$ produces a relatively more severe adverse pressure gradient in the diffuser and the flow separates there. Somewhere between these two cases, there exists a velocity distribution such that at every location the momentum of the boundary layer is just able to overcome the adverse pressure gradient so that the flow remains attached throughout the diffuser. This is called the optimum diffuser velocity distribution and is achieved when $b = 0.794$. For comparison, Stratford's optimum velocity distribution[24] is also presented in Fig. 12. Although not clearly evident from the figure, the present optimum velocity distribution is slightly more consevative at the beginning of the diffusion process than that of Stratford. Since Stratford's distribution is derived on the basis of zero skin friction throughout the diffuser, it can be considered as a limiting case. A design velocity distribution (besides having a safety margin against separation) should have a slightly more gradual start to the pressure rise (the deceleration of velocity) than that of Stratford. The present optimum velocity distribution has this characteristic and deserves further investigation as a potential attractive inlet design.

Concuding Remarks

An analysis method based on incompressible potential flow corrected for compressibility was described. Several sample calculations compared well with experimental data. The most recent applications include an inlet with a leading edge slat, an auxiliary inlet, and suction or blowing boundary layer control. An optimum diffuser velocity distribution was also developed. This paper shows that the present methods can be a very powerful tool for the analysis and the design of V/STOL inlets.

References

1. Stockman, N. O., and Farrell, C. A. Jr., "Improved Computer Programs for Calculating Potential Flow in Propulsion Systems Inlets," NASA TM-73728, 1977.

2. Albers, J. A., and Gregg, J. L., "Computer Program for Calculating Laminar, Transitional, and Turbulent Boundary Layers for a Compressible Axisymmetric Flow," NASA TN D-7521, 1974.

3. Hawk, J. D., Stockman, N. O., and Farrell, C. A. Jr., "Computer Programs for Calculating Two-Dimensional Potential Flow in and About Propulsion Systems Inlets," NASA TM-78930, 1978.

4. Hawk, J. D., and Stockman, N. O., "Computer Programs for Calculating Two-Dimensional Potential Flow Through Deflected Nozzles," NASA TM-79144, 1979.

5. Hess, J. L. Mack, D. P., and Stockman, N. O., "An Efficient User-Oriented Method for Calculating Compressible Flow in and About Three-Dimensional Inlets - Panel Method," Douglas Aircraft Co., Inc., Long Beach, CA., MDC-J7733, July 1979. (NASA CR-159578).

6. Herring, H. J., "PL2 - A Calculation Method for Two-Dimensional Boundary Layers with Cross-flow and Heat Transfer," Dynalysis of Princeton, Report Number 65, July 1980.

7. Shaw, R. J., Williams, R. C., and Koncsek, J. L., "VSTOL Tilt Nacelle Aerodynamics and its Relation to Fan Blade Stresses," NASA TM-78899, 1978.

8. Miller, B. A., Dastoli, B. J., and Wesoky, H. L., "Effect of Entry-Lip Design on Aerodynamics and Acoustics of High Throat Mach Number Inlets for the Quiet, Clean, Short-Haul Experimental Engine," NASA TM X-3222, 1975.

9. Burley, R. R., "Effect of Lip and Centerbody Geometry on Aerodynamic Performance of Inlets for Tilting-Nacelle VTOL Aircraft," AIAA Paper 79-0381, Jan. 1979.

10. Abbott, J. M., "Aerodynamic Performance of Scarf Inlets," AIAA Paper 79-0380, Jan. 1979.

11. Burley, R. R., Johns, A. L. and Diedrich, J. H., "Subsonic VTOL Inlet Experimental Results," Proceedings of Workshop on V/STOL Aircraft Aerodynamics, Volume II, Naval Post Graduate School, Moneterey, CA., edited by C. Henderson and M. F. Platzer, AD-A078909, 1979, pp. 648-664.

12. Johns, A. L. Williams, R. C., and Potonides, H. C., "Performance of a V/STOL Tilt Nacelle Inlet with Blowing Boundary Layer Control," AIAA Paper 79-1163, June 1979.

13. Kao, H. C., "Some Aspects of Calculating Flows About Three-Dimensional Subsonic Inlets," NASA TM-82678, 1981.

14. Smith, A. M. O., and Pierce, J., "Exact Solution of the Neumann Problem. Calculation of Non-Circulatory Plane and Axially Symmetric Flows About or Within Arbitrary Boundaries," ES-26988, Douglas Aircraft Co., ES-26988, Apr. 1958.

15. Hess, J. L., and Smith, A. M. O., "Calculation of Potential Flow About Arbitrary Bodies," Progress in Aeronautical Sciences, Vol. 8, D. A. Kuchemann, ed., Pergamon Press, Elmsford, NY, 1967, pp. 1-138.

16. Hess, J. L., "Calculation of Potential Flow About Bodies of Revolution Having Axes Perpendicular to the Free-Stream Direction," Journal of the Aerospace Sciences, Vol. 29, No. 6, June 1962, pp. 726-742.

17. Stockman, N. O., "Potential Flow Solutions for Inlets of VTOL Lift Fans and Engines," Analytical Methods in Aircraft Aerodynamics, NASA SP-228, 1970, pp. 659-681.

18. Lieblein, S., and Stockman, N. O., "Compressibility Correction for Internal Flow Solution," Joural of Aircraft, Vol. 9, No. 4, Apr. 1972, pp. 312-313.

19. Stockman, N. O., "Recent Applications of Theoretical Analysis to V/STOL Inlet Design," NASA TM-79211, 1979.

20. Herring, H. James, "Numerical Calculations of Slot Injection in a Two-Dimensional Boundary Layer," Dynalysis of Princeton, Report No. 68, 1981.

21 Burley, R. R., and Hwang, D. P., "Experimental and Analytical Results of Tangential Blowing Applied to a Subsonic V/STOL Inlet," to be presented at AIAA/ASME/SAE 18th Joint Propulsion Conference, Cleveland, OH June, 1982. AIAA Paper No. 82-1084.

22. Boles, M. A., and Stockman, N. O., "Use of Experimental Separation Limits in the Theoretical Design of V/STOL Inlet," Journal of Aircraft, Vol. 16, No. 1, Jan. 1978, pp 29-34.

23. Luidens, R. W. Stockman, N. O., and Diedrich, J. H., "Optimum Subsonic, High-Angle-of-Attack Nacelles," ICAS Proceedings 1980, 12th Congress of the International Council of the Aeronautical Sciences, edited by J. Singer and R. Staubenbiel, AIAA, 1980, pp. 530-541.

24. Straford, B. S., "The Prediction of Separation of the Turbulent Boundary Layer, "Journal of Fluid Mechanics, Vol. 5, Jan. 1959, pp. 1-16.

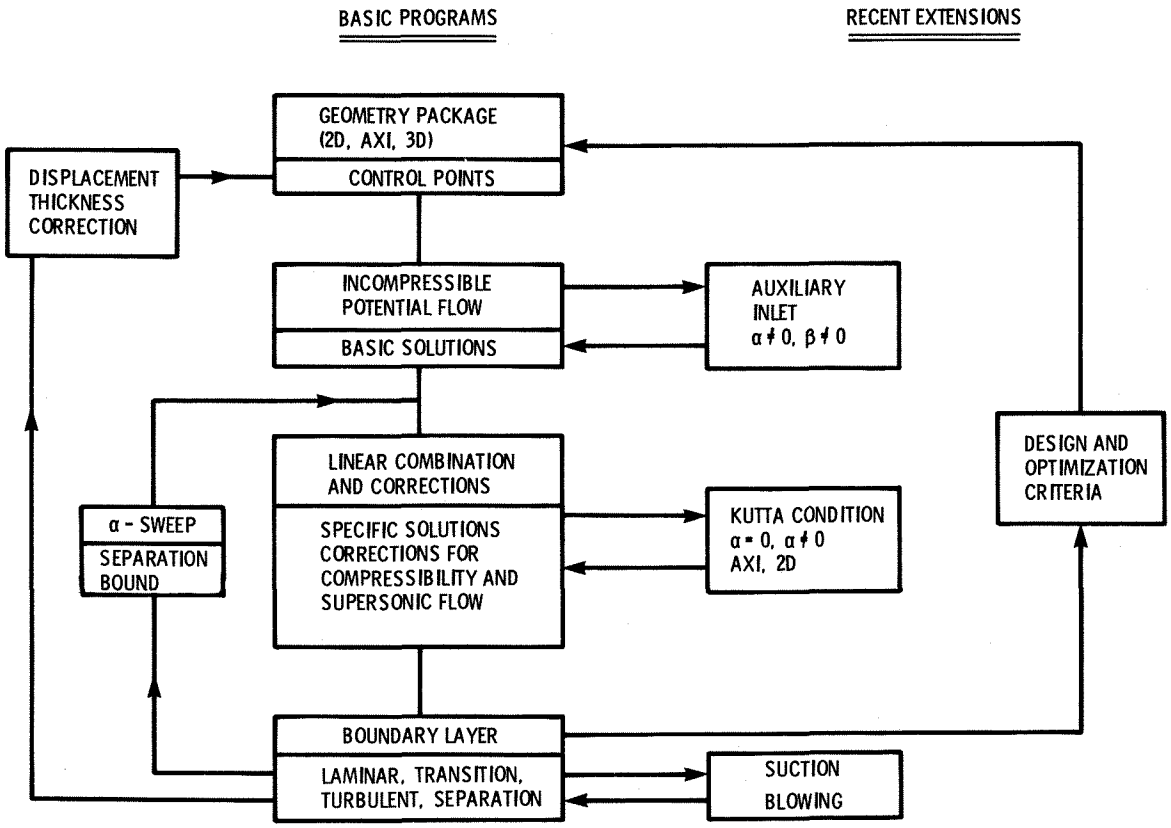

Figure 1. - Schematic diagram of computer programs.

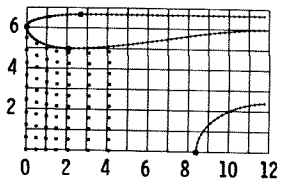

(a) 2D or axisymmetric inlet.

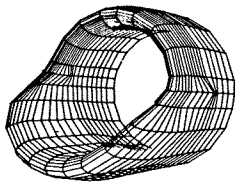

(b) Three-dimensional inlet.

Figure 2. - Inlet geometries.

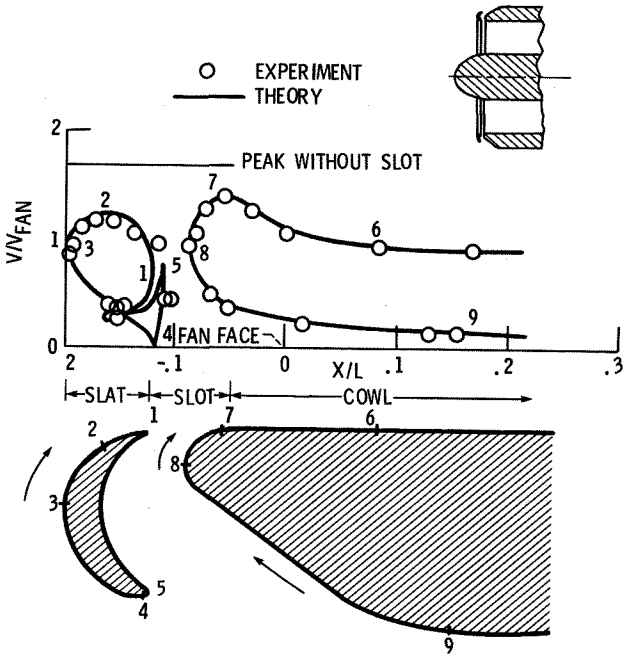

Figure 3. - Short inlet with a leading edge slot, $V_0 = 0$.

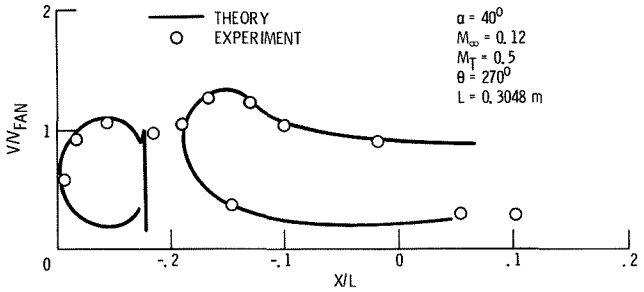

Figure 4. - Short inlet with a leading edge slot at angle of attack.

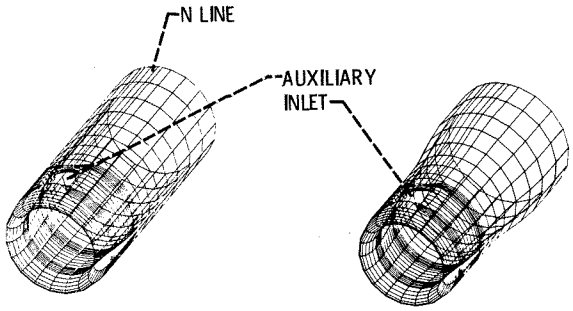

(a) NON-FLARED. (b) FLARED.

Figure 5. - Geometries required to obtain static solution for an inlet with auxiliary inlet.

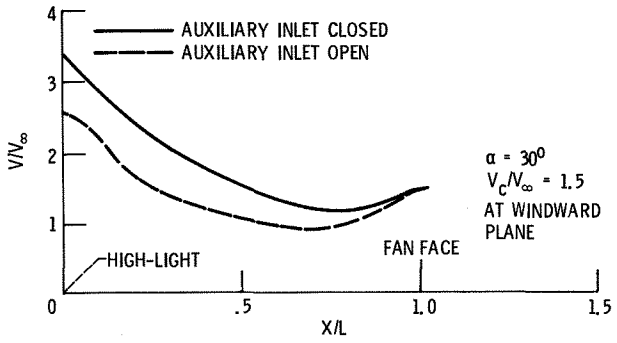

Figure 6. - The reduction of peak velocity by opening auxiliary inlet.

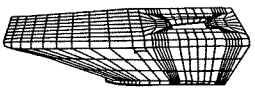

(a) Geometry.

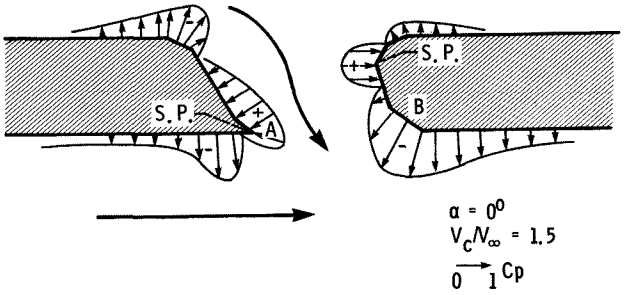

(b) Distribution of pressure coefficient along auxiliary inlet surface in the plane of symmetry.

Figure 7. - Supersonic inlet with top auxiliary inlet.

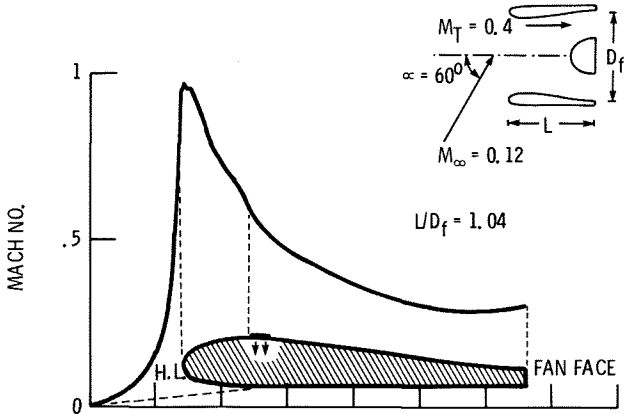

$\frac{\dot{m}_{suction}}{\dot{m}_{inlet}} = 0.12\%$ $\frac{p_s}{P_o} = 0.796$

NO SUCTION
SUCTION

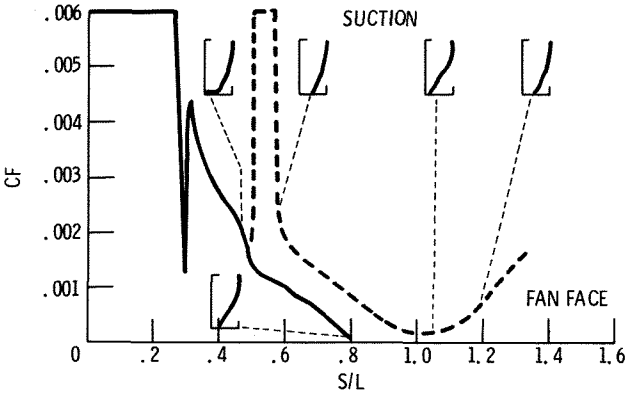

Figure 8. - Skin friction and velocity profiles with and without suction.

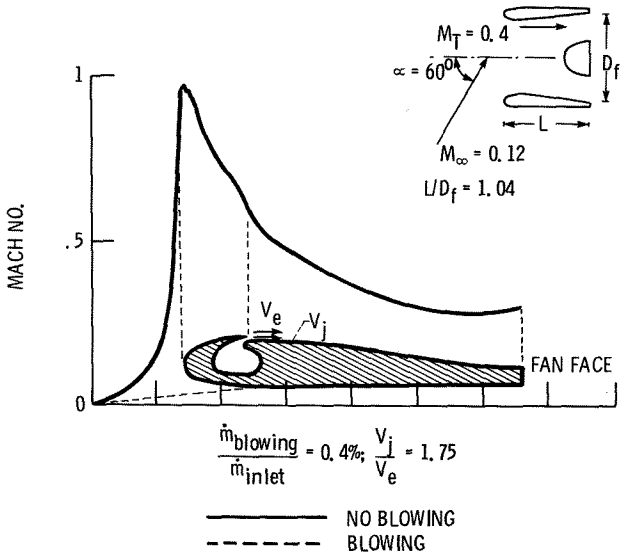

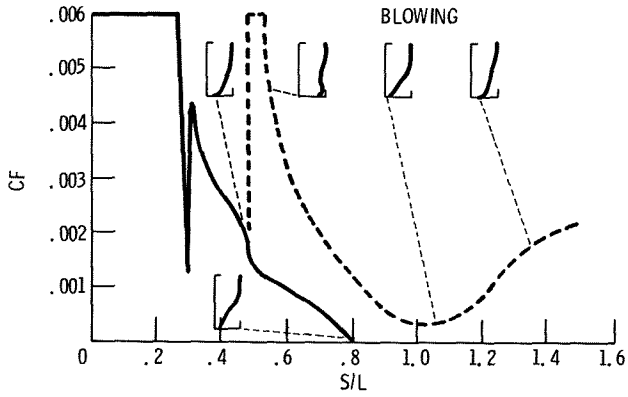

Figure 9. - Skin friction and velocity profiles with and without blowing.

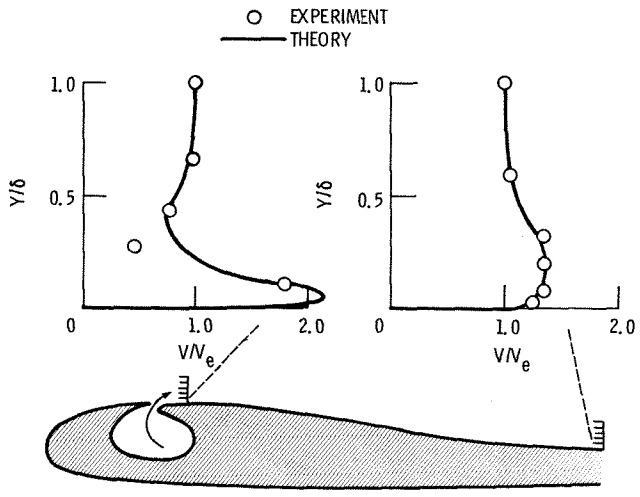

Figure 10. - Comparison of analytical and experimental velocity profiles. Windward plane, $\alpha = 70^0$, $V_T/V_\infty = 2$, $P_B/P_\infty = 1.2$.

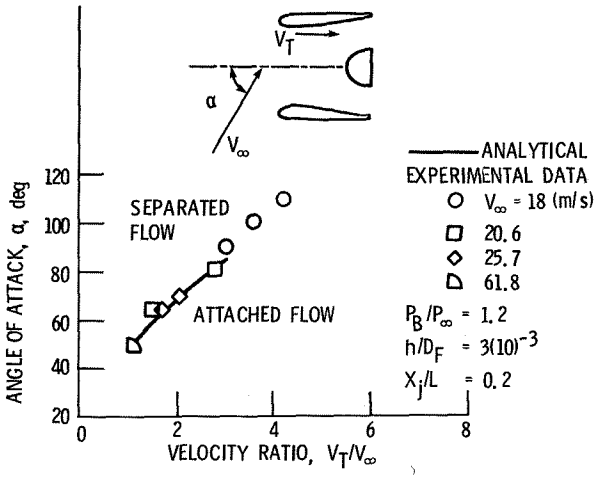

Figure 11. - Comparison of analytical and experimental separation bounds for blowing boundary layer control.

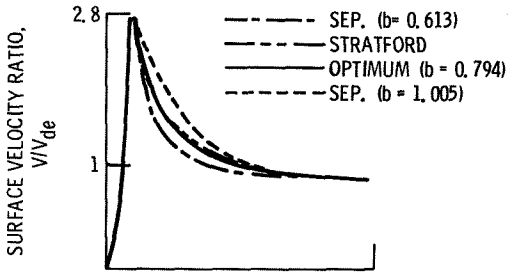

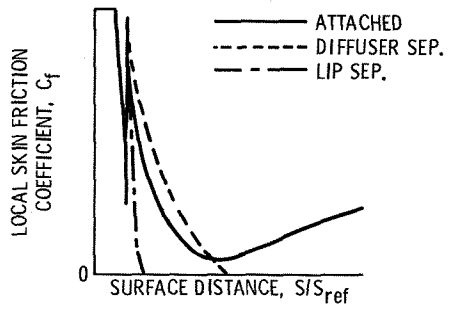

Figure 12. - Optimum velocity distribution.